Analysis and Design of Capacitive Power Transmission System Employing Out-of-band Wireless Feedback Link

Sung-Jin Choi and Hee-Su Choi
School of Electrical Engineering
University of Ulsan
Ulsan, 44610, Korea
E-mail: sjchoi@ulsan.ac.kr

***Abstract*— Capacitively-coupled wireless power transmission utilizes electric field applied between physically separated metal plates. Especially in full wireless power system which has no battery inside the target object, how to provide the regulated output voltage through the resonant LC link are challenging task. In this paper, analysis and control design of such system are investigated. Transfer function of the overall system including feedback delay latency is analyzed and control loop is designed in the frequency domain. The theoretical results are verified by PSIM simulation.**

I. INTRODUCTION

Capacitive wireless power transmission (C-WPT) utilizes the electric field applied between the physically separated metal barriers. The link capacitance formed between both sides of the barrier provides the ac current path through the barrier, but it should be cancel out by series resonant inductor to improve the efficiency and thus the overall circuit with transmitter and receiver forms resonant converter [1]. However, most of the works on the system has been about the circuit topology and there are few works on its control issue. The reason is because they mainly consider battery charging application. When the battery is present in the receiver circuit, the control doesn't need to be as tight and fast as most power supplies are.

Considering all aspects of the emerging wireless power technology, wireless power application can be divided into two groups. First one is hybrid wireless power system which admits intermittent power transmission because the receiving object already has sufficient battery back-ups therein. Applications such as charging stations for cell phones, tablets, vacuum cleaners, or robot cleaners fall into this group. In these products, battery itself has an inherently large time constant caused by chemical reactions and does not need fast control. It needs just power flow control of charging sequence between the constant current/constant voltage (CC/CV) modes whose time constants are more than a few tens of minutes [2,3].

On the contrary, the other application which needs continuous power transmission through the wireless energy link can be categorized as full wireless power system. It has no battery inside the target object. Therefore, regulating the output voltage in the receiver are challenging task to be investigated. Moreover, because the transmitter and receiver are physically separated, the control loop should be implemented by the wireless feedback link.

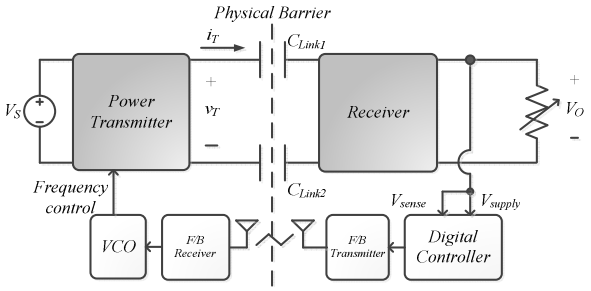

Fig. 1. Full wireless power system based on C-WPT

In this paper, in order to obtain the regulated output voltage in the absence of battery power in the target object, the guideline for the control loop implementation for the C-WPT system has been studied.

II. SYSTEM DESCRIPTION

Figure 1 shows the block diagram of the target system. It consists of transmitter, receiver, capacitive energy link, feedback (F/B) controller, wireless signal link, gate drive circuitry. Being a resonant converter, the system adopts frequency control where the switching frequency is adjusted by voltage-controlled oscillator (VCO)[4]. The dotted line in the center of the figure depicts the physical barrier between the transmitter and the receiver.

In this paper, the half bridge structure with double matching transformers [5] in Fig. 2 has been adopted. In this configuration, transmitter contains two power MOSFETs turning on alternatively with 50% duty cycle to provide the ac voltage waveforms. The series inductor, L_r, compensates the reactance of the effective link capacitance, C_e which is formed by the series connection of C_{Link1} and C_{Link2}, and the input

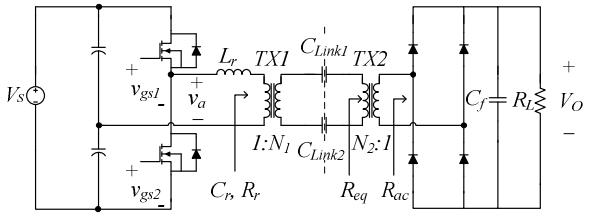

Fig. 2. Power stage topology

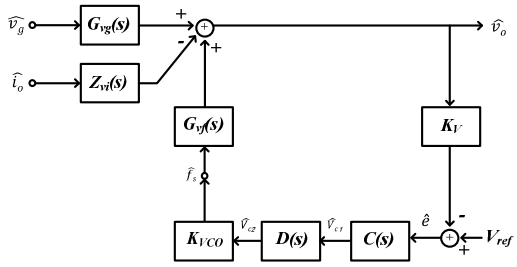

Fig. 3. Control block diagram

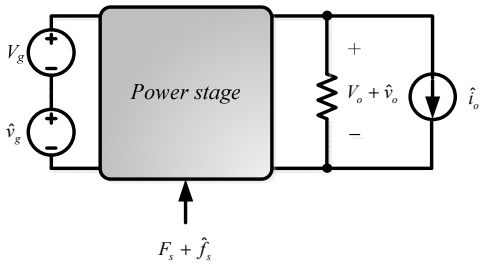

Fig. 4. General method to model resonant converters

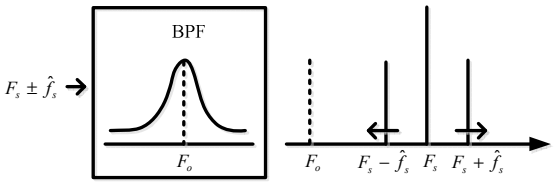

Fig. 5. Frequency modulation and beat frequency

transformer, TX_1 provides the impedance matching to provide zero voltage turn-on features to the main switches. The output matching transformer, TX_2 is adopted to increase the effective output load impedance seen by LC resonant tank. Meanwhile, the resonant waveforms are restored to dc voltage on the load resistance, R_L, by the full-wave rectifier with the output filter capacitor, C_f, in the receiver circuit. Therefore, the overall power stage constitutes a series resonant converter.

Because there is no additional post-regulator or active rectifier in the receiver unit, once the feedback controller generates a control voltage from the error signal between the reference voltage and the sensed voltage, it returns back to the transmitter side by the F/B transmitter-receiver pair. Though it has been shown that feedback signal can be fed back to transmitter side by in band communication where the signal is modulated by the main power waveforms such as in load modulation technique [6], extraction of the modulated signal may not be reliable in the wide operating frequency variation. For these reasons, this scheme is not further investigated, and this paper only studies out-of-band wireless feedback which uses frequency band different from that used in the main power transmission.

III. Analysis and Modeling

The control block diagram of the overall system is shown in Fig. 3. In the figure, $G_{vf}(s)$ is the control to output transfer function, $Z_{vi}(s)$ is output current to voltage transfer function, and $G_{vg}(s)$ is the input voltage to output transfer function of the power stage. K_V is the feedback sensing gain, K_{VCO} is the gain in the voltage controlled oscillator, and C(s) is the compensator block to be designed here. D(s) models the delay latency of the wireless feedback link. The loop gain of the negative feedback system is

$$T(s) = K_{VCO} \cdot K_V \cdot G_{vf}(s) \cdot D(s) \cdot C(s) \quad (1)$$

In order to design the control loop, the individual blocks are analyzed in this section.

A. Forward path : power stage

The modeling of the power stage is performed by injecting small signal perturbation to the power stage as shown in Fig. 4. Especially, the small-signal model of series resonant converters has been investigated either theoretically [7] or heuristically [8]. However, the former is too complex to use and the latter only deals with control to output transfer function. Therefore, in this paper, after the swept sine analysis in PSIM [9] is applied to extract the power stage transfer functions, the salient pole-zero locations are identified by curve fitting algorithms.

Salient pole and zero locations are justified heuristically by the high Q approximation as follows. By time constant analysis, we can expect presence of low frequency pole caused by low filter action of the output capacitor, C_f. It has been also shown in [8] that the LC resonant tank acts as a high pass filter and generates additional two more poles into the system which is given by the beat frequency between the bias switching frequency, F_S, and the resonant frequency, F_o. This kind of frequency modulation phenomena is explained in Fig. 5. For example, when the switching frequency is perturbed with a modulation frequency, there will be a side band in the response of the driving frequency and resonance phenomenon occurs in that beat frequency. If F_s is well above F_o, the system can be approximated as a first order system in the control bandwidth of concern. Such a dominant pole assumption fails if F_s is very close to F_o. In this case, control to output transfer function $G_{vf}(s)$ will be given by the third order system given by

$$G_{vf}(s) = \frac{G_{vf,o}}{\Delta(s)} \tag{2}$$

where $G_{vf,o}$ is the dc gain and $\Delta(s)$ is the system characteristic polynomial as in in the following.

$$\Delta(s) = \left(1 + \frac{s}{\omega_{pf}}\right)\left(1 + \frac{s}{Q\omega_{pn}} + \frac{s^2}{\omega_{pn}^2}\right) \tag{3}$$

As is mentioned above, the low frequency single pole is caused by the output filter, and the 2nd order pole occurs at the beat frequency. Thus it is reasonable to think those pole locations are

$$\omega_{pf} \approx \frac{1}{C_f(R_L \,||\, G_{vi,o})} \tag{4}$$

$$\omega_{pn} = \omega_s - \omega_o \tag{5}$$

In the above calculation, $G_{vi,o}$ is dc gain of the current-to-output transfer function.

B. *Return path : control signal*

In the frequency controlled system, VCO gate pulses and determines the switching frequency. Small signal transfer gain of VCO can be modeled by the following formula.

$$K_{VCO} = \left.\frac{df_s}{dv_{c2}}\right|_{f_s = F_s} \approx \frac{F_{s,\max} - F_{s,\min}}{V_{c2,\max} - V_{c2,\min}} \tag{6}$$

where $F_{s,max}$ and $F_{s,min}$ is the maximum and minimum of the possible frequency span and $V_{c2,max}$ and $V_{c2,min}$ is the corresponding input voltage of VCO used in the system.

After a control voltage is generated in the feedback controller from the error signal between the reference voltage and the sensed voltage, it returns back to the transmitter side by the wireless feedback link. Assume the communication is stable and reliable, the latency introduced in the wireless link is modeled by a time delay function

$$D(s) = e^{-s\tau} \approx \frac{1 - s\tau/2 + (s\tau)^2/12}{1 + s\tau/2 + (s\tau)^2/12} \tag{7}$$

where τ is the average delay time of the communication channel and herein is used the second order Padé approximation [10]. It approximates the delay effect as an all-pass-filter which introduces two poles and two right-half-plane (RHP) zeros. Because of the additional strong phase drop it causes, the delay time will mainly determine the control loop bandwidth.

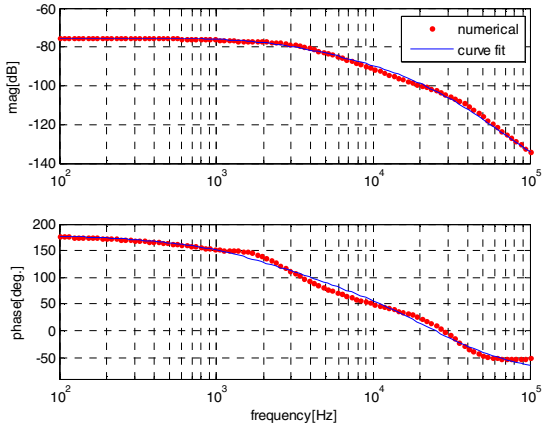

Fig. 6. Control to output transfer function, $G_{vf}(s)$

TABLE II. TRANSFER FUNCTION PARAMETERS

Parameter	$G_{vf}(s)$			
	$G_{vf,o}$	ω_{pf} (krad/s)	ω_{pn} (krad/s)	Q
Value	1.75×10^{-4}	$2\pi\cdot2.24$	$2\pi\cdot22.7$	0.519

Assume the switching frequency is designed well above the resonant frequency and the load quality factor is sufficiently high, the overall loop gain can be approximated by a single pole system when the delay time is relatively small. On the contrary, if the feedback wireless link suffers severe latency, it can be approximated by double pole and double right-half-plane zero system.

In the former case, a type-2 or PI compensator is enough and its compensator zero is placed to cancel out the power stage pole. Then the loop crossover is placed well below both $1/\pi\tau$ and f_{pn} to prevent additional phase lag and avoid conditional stability situation which may deteriorate the phase margin in the loop gain. If the control crossover frequency, f_C is selected, k_p and k_i of the PI compensator are determined by

TABLE I. SYSTEM PARAMETERS

Parameter	V_s	V_o	I_o	F_s	F_o	Q_o	C_e	L_r	N_1	N_2	C_r	K_{vco}	K_v
Value	19	10	0.5	293	280	1.92	272	21.8	7.5	4.3	10	95.7	1
Unit	V	V	A	kHz	kHz	Ω/Ω	pF	uH			uF	kHz/V	V/V

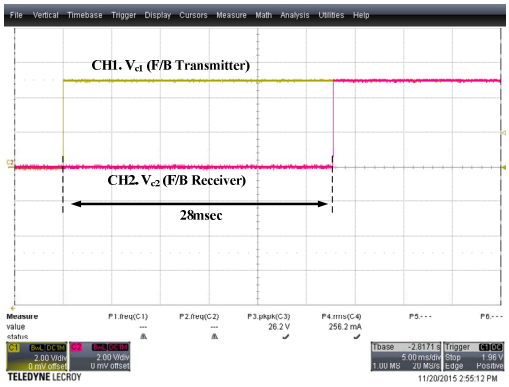

Fig. 7. Measurements of delay in the Bluetooth feedback link (Ch1 : V_{c1} (F/B Transmitter), Ch2 : V_{c2} (F/B Receiver))

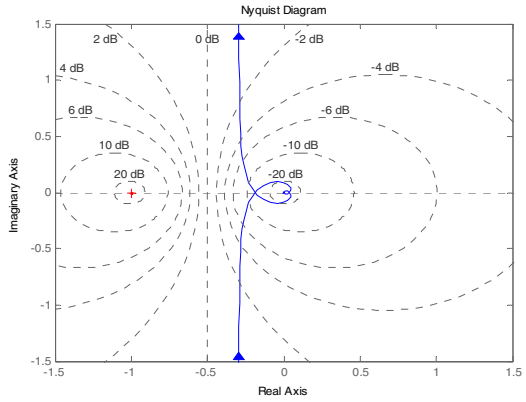

Fig. 8 Nyquist diagram of T(s)

$$k_i = \frac{2\pi f_C}{K_{VCO} G_{vf,0} K_V}, \quad k_p = k_i (R \,||\, G_{vi,0}) C_f \tag{8}$$

However, the latter case needs a type-3 controller placing two compensator zeroes to cancel out both the power stage pole and the delay pole.

IV. Design and Implementation

The power stage has been designed to transmit 5W power through a pair of square plates with dimension of 10cm x 10cm separated by 0.15mm air gap and supplies the output voltage of 10V up to 0.5A load current. Table I shows the parameters used in the system construction.

Using the circuit parameter shown in Table I, PSIM schematic has been constructed and transfer functions of the power stage have been extracted by ac sweep analysis. After simulation has been done, pole-zero locations are identified by curve fitting algorithm [11] and are summarized in Table II. The theoretical study on the power stage transfer function given by Eqs. (2)-(5) predicts that the low frequency pole and the high frequency natural poles exit in 2.24kHz and 22.7kHz, respectively. Fig. 6 compares two $G_{vf}(s)$'s obtained by the swept sine analysis and the theoretical predictions, where both results show good agreement.

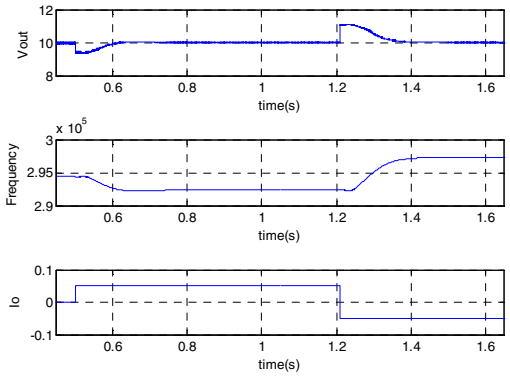

Fig. 9. Output voltage responses to load step changes: simulation

Meanwhile, the wireless feedback link has been implemented in Serial Port Profile (SPP) of Bluetooth 2.1 protocol compatible with IEEE 802.15.1[12]. The serial communication in 115,200 bps introduces about 87usec delay. However, because of an additional delay caused by internal polling mechanism, its minimum bound is reported as large as 12~13ms [13]. This delay effect can be observed in the hardware results shown in Fig. 7 and hence τ=35msec is used in this paper. Incorporating the double pole and double RHP zero at 16Hz introduced by the wireless link latency, designed compensator provides the f_C=1.33Hz with phase margin of 73.1 degree and gain margin of 14.6dB at the full load condition.

Fig. 8 shows the Nyquist plot of the loop gain, T(s), including the controller that has been designed. Fig. 9 shows the step response when the load current is slightly increased by 10% and then decreased by 10% from the 0.5A full load condition, and the system shows good performance in the output regulation.

V. Conclusions

This paper has analyzed the C-WPT system which involves resonant power link and out-of-band feedback link to regulate the output voltage even without battery in the target object. The practical delay effects are modeled and included in the compensator design. The performance has been verified by PSIM simulation.

Acknowledgement

This research was supported by Basic Science Research Program through the National Research Foundation of Korea (NRF) funded by the Ministry of Education (grant number: NRF-2014R1A1A2059772).

References

[1] C. Liu, A. P. Hu, and N. K. C. Nair, "Modelling and analysis of a capacitively coupled contactless power transfer system," *IET Power Electronics*, vo1. 4, no. 7, pp. 808-815, 2011.

[2] T. Diekhans and R. W. De Donker, "A Dual-Side Controlled Inductive Power Transfer System Optimized for Large Coupling Factor Variations and Partial Load, *IEEE Transactions on Power Electronics*, Vol. 30, No. 11, pp. 6320-6328, Nov., 2015.

[3] C.-G. Kim, D.-H. Seo, J.-S. You, J.-H. Park, and Bo H. Cho, "Design of a Contactless Battery Charger for Cellular Phone," *IEEE Transactions on Industrial Electronics*, vol. 48, no. 6, pp. 1238-1247, 2001.

[4] R. Rosshard, U. Badsübner, J. W. Kolar, and I. Stevanovic, "Comparative evaluation of control methods for inductive power transfer," *Proceedings of ICRERA*, 2012, pp.1-6.

[5] S.-J. Choi and H.-S. Choi, "Capacitive Wireless Power Transfer System with Dobule Matching Transformers for Reduced Stress and Extended ZVS Range," *IEEE INTELEC 2015*, Oct., pp.791-796.

[6] K. Finkenzeller, *RFID Handbook: Fundamentals and Applications in Contactless Smart Cards and Identification*, 2_{nd} ed. Wiley & Sons, 2003.

[7] A. F. Witulski and R. W. Erickson, "Small Signal Equivalent Circuit Modelling of the Series Resonant Converter," *IEEE PESC 1987 Record*, pp. 693-704.

[8] V. Vorperian, "Approximate Small-Signal Analysis of the Series and the Parallel Resonant Convertes," *IEEE Transactions on Power Electronics*, vol. 4, no. 1, Jan. 1989.

[9] POWERSIM, *PSIM User's Guide*, ver. 9, May, 2010.

[10] J. R. Partington, "Some Frequency-domain Approaches to the Model Reduction of Delay Systems," *Annual Reviews in Control*, vol. 28. pp. 65-73, 2004.

[11] Levi, E. C. "Complex-Curve Fitting," *IRE Trans. on Automatic Control*, vol. AC-4, pp. 37–44, 1959.

[12] Bluetooth SIG , *Bluetooth 2.1 Specification*, https://www.bluetooth.org/

[13] M.J. Moron, R. Luque, E. Casilari and A. Diaz-Estrella, "Minimum Delay Bound in Bluetooth Transmissions with Serial Port Profile," *Electronics Letters*, vol. 44, pp.1099-1100, Aug., 2008.